Phenomenology of Passive Broadband Terahertz Images

Charles Dietlein[1], Arttu Luukanen[2], Francois Meyer[1], Zoya Popovic[1], and Erich Grossman[3]

[1]*University of Colorado at Boulder*
Department of Electrical and Computer Engineering
425 UCB, Boulder, CO, 80309-0425, U.S.A.
Email: dietlein@colorado.edu

[2]*VTT Information Technology*
Millimetre Wave Laboratory
P.O. Box 1202, Tietotie 3, Espoo, 02044 VTT, Finland
Email: arttu.luukanen@vtt.fi

[3]*National Institute of Standards and Technology*
Optoelectronics Division
325 Broadway, Boulder, CO, 80305-3328, U.S.A.
Email: grossman@boulder.nist.gov

Abstract
Images acquired by a 105-mK noise equivalent temperature difference (NETD) scanned single-pixel broadband 0.1–1 THz passive system are analyzed with two specific parameters of interest in mind. First, the minimum system noise level for clothing feature extraction and concealed weapons detection is determined empirically by measuring the temperature differences created by clothing folds/ripples and ceramic/metallic weapons, and adding specific levels of noise to the image. Second, the effective spatial resolution of the images is found by examining the transition between temperature regions throughout the scene and finding the effective frequency of operation via theoretical edge diffraction.

Keywords: superconducting, passive imaging, terahertz, effective spatial resolution, feature detection

1. INTRODUCTION

This paper presents phenomenological analysis of images obtained by mechanically raster-scanning a single-pixel superconducting antenna-coupled microbolometer over a scene. The device is a novel cryogenically-cooled (4 K) vacuum-bridge Nb microbolometer, coupled to a logarithmic spiral antenna with a bandwidth from 0.1–1.1 THz. A voltage bias is applied to the arms of the spiral antenna, and the resulting current decrease through the bolometer upon incident radiation is sensed by a low-noise room-temperature readout circuit. The device has high sensitivity and low noise, i.e., noise equivalent power, NEP = 25 fW/Hz$^{1/2}$ and NETD = 105 mK referenced to a lock-in amplifier time constant of 30 ms. Each image in this paper takes approximately 20 minutes to acquire; the integration time per pixel is 10 ms, and the number of pixels in each image is 12,000–14,000. The majority of the acquisition time is occupied by the mechanical scanning of the primary collecting aperture, a 30-cm diameter spherical mirror mounted on a two-axis servo stage. A complete description of the bolometer, optics, and amplification circuitry is found in [1].

Images presented are acquired in an uncontrolled indoor lab scene, with various equipment, lights, windows, and other sources of temperature fluctuations present in the background of the room. Therefore, the focus of this analysis is on the target of the imaging system, that is, a human approximately 1 m from the primary collecting aperture of the system optics. The images are unprocessed, i.e., each pixel represents incident irradiance. Because concealed weapons detection is one of the possible and attractive applications of passive terahertz imaging, a concealed threat object (a ceramic knife or metal gun) is shown in each of the images. Objects in a scene, concealed or otherwise, are identified by their radiometric temperature contrast with either (1) other objects in, or (2) the background of, the scene. The radiometric temperature, T_{rad}, of an object is typically approximated by the following formula:

$$T_{rad} \approx \varepsilon T_{obj} + (1-\varepsilon) T_{bg} \ , \qquad (1)$$

where ε is the emissivity of the object, and the *obj* and *bg* subscripts represent the object and the background, respectively. In an indoor scene, the radiometric temperature contrast between objects and the background is low, compared to an outdoor scene. Between a human and room temperature, which is generally the largest temperature

contrast found indoors, the temperature difference is only 15 K. The radiometric temperature contrast between threat objects and the human concealing them is less than 10 K.

This paper is divided into two topics. First, the minimum NETD for detection of certain features is explored. This is accomplished by systematically adding Gaussian noise to the image until features are obscured by noise. Adding Gaussian noise to an image with low noise is effectively the same as acquiring an image with a noisy system or detector, so we can determine the minimum NETD required for specific information in an image to be detected. The second topic is the effective frequency of operation. The spatial resolution is proportional to the frequency, but in a broadband system the frequency is not well-defined. By applying diffraction theory, the effective frequency and therefore the diffraction-limited resolution is found.

2. IMAGE NOISE

The image noise, i.e., the standard deviation, can be directly measured in images we acquire since the scene temperature fluctuations are above the NETD of the device. The measured NETD in the images ranges from 150–300 mK in small regions of interest representing several square meters of quasi-uniform, yet still uncontrolled, background. Also easily measured is the radiometric temperature difference between natural folds or ripples in clothes (corresponding to directly adjacent to the human body and several cm away from the body), and between human and the concealed threat object.

Because the system is both sensitive enough and has a low NETD, the images provide a valuable baseline for making phenomenological statements about the required specifications for other systems or devices. That is to say, with a certain system NETD, a certain confidence level is attained for the ability for the system to view varying levels of detail in the images. Fig. 1(a) is an image with a measured NETD of approximately 0.2 K in the background. Fig. 1(b) shows the temperature profile along the white line in Fig. 1(a); the folds in the clothing (e.g. the sleeve on the left side of the image) create a temperature variation of 1–3 K, while the concealed ceramic knife creates an 8 K difference. The feature in the center of the image is due to a thick collar where four layers of material overlap, for a 5 K temperature difference. Basing image quality on features such as folds in clothes or clothing shadows is subjective, yet there is a standard term applied to these natural attributes which we see everyday with visible light, and that is "scene clutter." When natural scene clutter exists in a THz image such as Fig. 1, it becomes easier for our eyes and associated signal processing to detect objects which are out of place. When the scene clutter is obscured by noise, it becomes more difficult to trust that our eyes are indeed detecting a concealed threat object and not a noisy feature which, in a noise-free image, could be natural clutter which we are used to observing.

To determine how an increased NETD conceals the features that make this image look subjectively "good", Gaussian white noise is added to the image, where the standard deviation (σ) of the Gaussian function is equal to the NETD of the noise. Setting σ to values corresponding to features in the image and viewing the images allows subjective determination of whether or not a certain feature is concealed by the added noise. Because the noise is uncorrelated with existing noise in the image, the total σ in the same region of the background where the original noise measurement was taken is approximately equal to the added noise. That is to say, when Gaussian noise with $\sigma = 0.5$ K is added to an image with $\sigma = 0.2$ K, the total σ in the analyzed area of the image is approximately 0.5 K. Fig. 2 demonstrates addition of Gaussian white noise to the image of Fig. 1(a). It is seen that as Gaussian white noise is added to the images in with σ equal to ΔT corresponding to features shown in Fig. 1(b), the features themselves become undetectable. The noise in Fig. 2(a) decreases the visibility of the clothing folds on the left, while any features noticed on the right are obscured completely. Similarly, in Fig. 2(b), the folds are hard to identify without previous knowledge of their existence. In Fig. 2(c), it is difficult to differentiate between the concealed weapon and the clothing feature. Finally, without *a priori* information about Fig. 2(d), knowledge of a concealed weapon is non-existent. Although the ceramic knife registers as a cooler area, in no way can a definitive statement be made about what it is.

3. SPATIAL RESOLUTION

Four-bar spatial resolution targets and a novel method of temperature calibration utilizing an optical trap design are currently being developed for systematic measurement of the system (combined optics and detector) modulation transfer function (MTF). The MTF is a standard measurement of spatial resolution [2], and the end product and test methodology will provide important results about the performance of this broadband system. A model for concealed weapon identification for terahertz imaging systems, based on component MTFs, has been proposed [3] and a similar performance metric will be implemented once our resolution and calibration system is complete. As the resolution targets are not yet available to us, another method of finding the effective spatial resolution is possible.

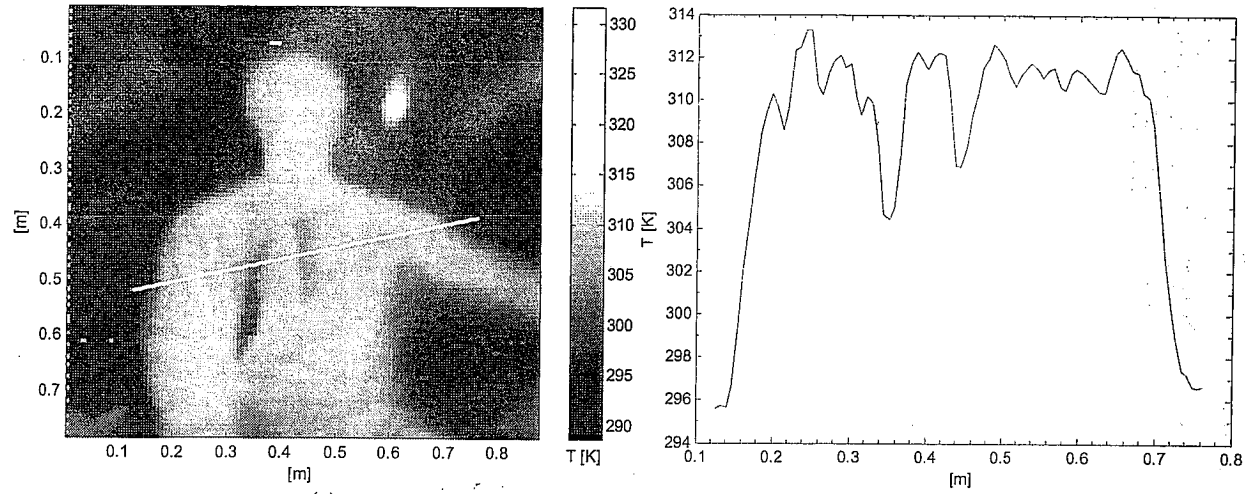

Fig. 1. (a) Image with measured NETD = 0.2 K in the background, and a ZrO_2 knife concealed under two layers of clothing; (b) Cut through image (white line in (a)) showing temperature variations. Folds in clothing correspond to ΔT between 1–3 K, while the knife shows an 8 K difference. The clothing feature in the center creates a difference of 5 K.

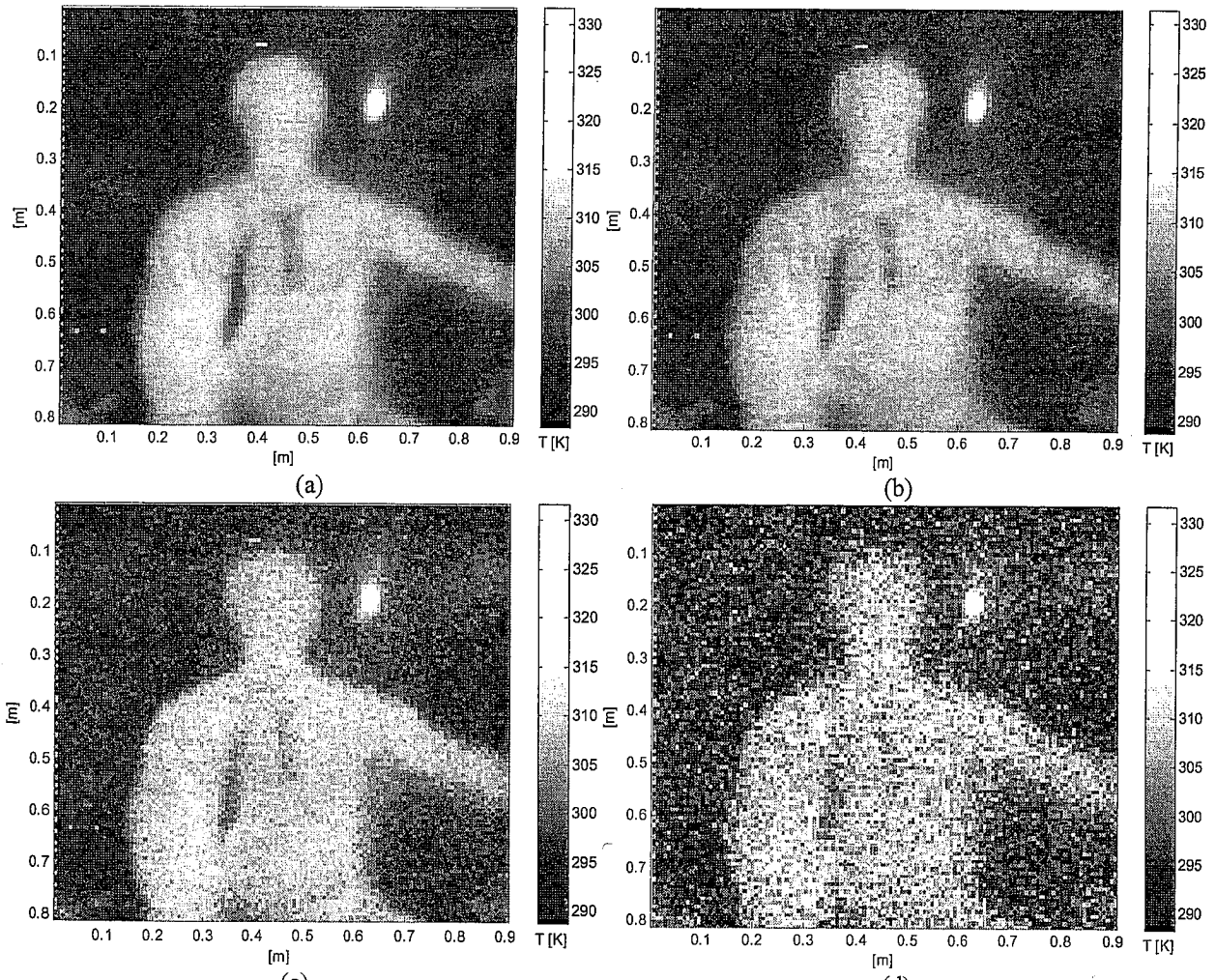

Fig. 2. Images with added Gaussian white noise, for NETD levels greater than seen in Fig. 1. (a) NETD = 0.5 K; (b) NETD = 1 K; (c) NETD = 2 K; (d) NETD = 5 K.

Because the system bandwidth covers a decade, spatial resolution is not well-defined. It is desirable to understand the effective frequency of operation which determines the resolution in the image, besides the scan-limited performance based on spatial dimensions of a pixel. One method of achieving this goal is to measure the transition between the target and the background along an edge, which is ideally a step function, and compare the non-ideal step slope with the slope found in diffraction theory. Due to the raster-scanning nature of the system optics, the vertical and horizontal spatial resolution will not be the same. The raster scanning in these images is row-based, where completion of a single row scan requires approximately fifteen seconds. The vertical resolution suffers due to small movements of the human being imaged, as the time required to scan through a vertical rectangular region along an edge is longer than the time required for a horizontal edge. In Fig. 3, an image is shown in which both a ceramic knife and a metallic gun are imaged. The white-outlined areas represent the approximately vertical and horizontal areas chosen for analysis. After selection of the desired area, the data is interpolated with a bicubic spline in order to rotate it into a rectangular matrix for averaging along the length of the rectangle. The outlined areas are only representative of the data used; several areas are measured from different images and the mean of the horizontal and mean of the vertical transitions are analyzed.

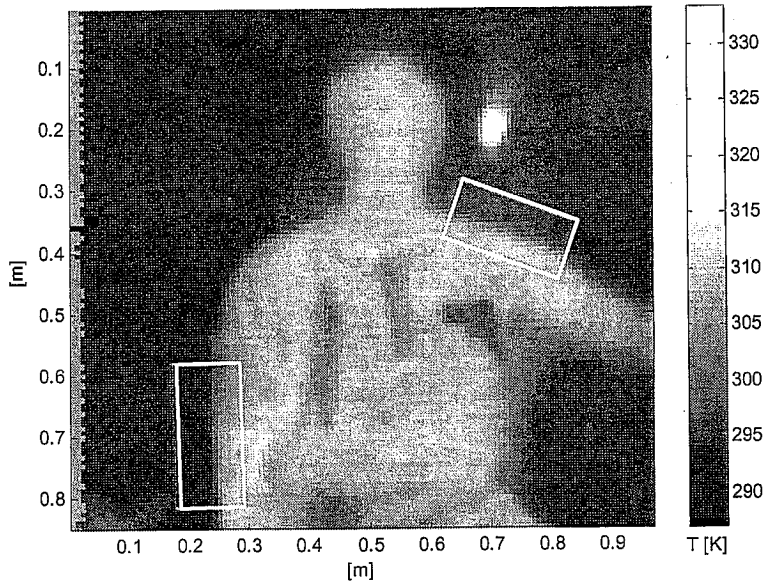

Fig. 3. An image for edge resolution analysis, containing a ceramic knife and a small metallic handgun. Examples of the analyzed regions are outlined in white.

It is seen in Fig. 4 that the lower half of the measured edge transition curves indeed match diffraction theory at a frequency of 400 GHz. For the upper half of the measured curve, no decaying ringing is seen as in edge diffraction, but the asymptotic approach to the maximum magnitude occurs at the same rate. A reasonable conclusion can be made, which is that although the system is basically a radiometer, the end data of interest is an image, much like a thermal camera provides. A thermal profile is therefore observed for the upper region of the curve, where the maximum temperature reached is inset from the edge of the body. The decaying ringing is due to the finite and sharp cutoff frequency; as the cutoff frequency is increased, the maximum amplitude decreases, and the ripple period increases. Eventually a step function is realized [4]. Also noted is that the asymptotic approach to the maximum normalized temperature can vary between areas of the image, due to the reflected background temperature varying by several K between the ceiling of the lab and the walls. This causes a more rapid increase for the horizontal edge where the majority of the reflected background is the ceiling, while for the vertical edge the walls are the major contributor of reflected background temperature. The raster scanning can introduce another resolution limit due to the velocity of the servo motor; if the horizontal scanning of the primary aperture is too rapid for the combination of samples per second and the integration time of the lock-in amplifier, blur between adjacent horizontal pixels will be a limiting factor. However, the lock-in amplifier time constant was set to be significantly low enough with respect to the sample rate and servo speed such that each sampled pixel is distinct from its most recently-sampled pixel neighbor.

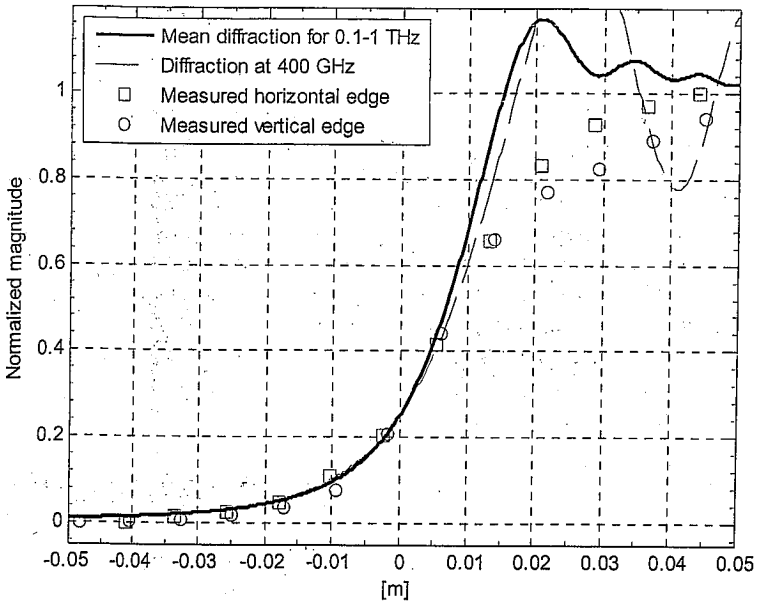

Fig. 4. Normalized magnitude of measured magnitude along the edge sections represented in Fig. 3, and theoretical diffraction curves for the same optics.

4. CONCLUSION

We have presented phenomenological analysis of passive indoor terahertz imagery. It has been shown that the minimum NETD for effective concealed object detection is 1 K in unprocessed images. Above 1 K, the noise obscures the scene clutter which allows both humans and computers to adequately process the image for conclusive object detection. This NETD was suggested in [1] and has now been empirically confirmed, due to the availability of a detector with ~100 mK sensitivity. Resolution performance can be reduced to three components. First, the method of scanning and timing of sampling and integrating can cause adjacent pixel blur. In the images shown here, however, the scan velocity was set low enough such that the integration for each pixel is completely distinct, i.e., integration is not overlapping for adjacent pixels. This is non-optimal and adds significant time to the acquisition, but the scanning effect becomes negligible. Second, diffraction theory shows a definite limit, which was identified. The resolution of the system is based on the f-number and effective frequency, which was found to be approximately 400 GHz based on the compared gradients from diffraction theory and measured edge transitions. The diffraction-limited resolution at the target distances in the images is 2.3 mm, but the spatial pixel size is greater than that limit. Finally, scene variation is a factor – both thermal drifts and human movement during the duration of the acquisition are parameters for which is it difficult to compensate.

Future work includes a circularly variable filter, a band-pass frequency-selective surface, for acquisition of images with spectral information as a third dimension, so the images can be analyzed spectrally. Additionally, the next version of this system will be video-rate, so scene and target variation will not be an issue due to the rapid acquisition of each frame.

5. REFERENCES

[1] A. Luukanen, A. J. Miller, and E. N. Grossman, "Passive hyperspectral terahertz imagery for security screening using a cryogenic microbolometer," *Proc. SPIE.*, vol. 5789, pp 127-134, May 2005.
[2] G. D. Boreman, *Modulation Transfer Function in Optical and Electro-Optical Systems*, SPIE Press Tutorial Texts in Optical Engineering: Bellingham, 2001.
[3] S. R. Murrill, E. L Jacobs, S. K. Moyer, C. E. Halford, S. T. Griffin, F. C. De Lucia, D. T. Petkie, and C. C. Franck, "Terahertz imaging system performance model for concealed weapon identification," *Proc. SPIE.*, vol. 5989, pp. 414-427, Nov. 2005.
[4] M. Born and E. Wolf, *Principles of Optics: Electromagnetic Theory of Propagation, Interference, and Diffraction of Light,* 7th ed., Cambridge University Press: Cambridge, pp. 565-578, 1999.